A Modeling-Based Technique for Nondestructive Evaluation of Metal Powders Undergoing Microwave Sintering

Alexander V. Brovko[1], Ethan K. Murphy[2], and Vadim V. Yakovlev[3]

[1]Saratov State Technical University, Saratov, 410070, Russia
[2]Rensellaer Polytechnic Institute, Troy, NY 12180, USA
[3]Worcester Polytechnic Institute, Worcester, MA, 01609, USA

***Abstract* — A microwave imaging technique is proposed for reconstruction of geometrical parameters (a spatial position and a radius) of a metal sphere emerging inside the sample of metal powder in the course of microwave sintering. The technique relies on a numerical inversion realized with an artificial neural network backed by data on *S*-parameters obtained from FDTD simulation and measurement. Numerical experiments are performed in the frequency range from 2 to 3 GHz for a cylindrical sample of iron powder in a two-port waveguide system. The results show that the spheres of not less than 2 mm radius are reconstructed with the average errors of 0.2-2.2%.**

***Index Terms* — FDTD methods, microwave imaging, neural network applications, nondestructive testing.**

I. Introduction

Microwave (MW) sintering of particulate materials is known to be an efficient alternative to conventional thermal sintering. Due to shorter processing time and lower sintering temperatures, materials produced by high temperature MW processing from ceramic, metal and composite powders can have improved microstructures and enhanced physical properties [1], [2]. The progress in upgrading of successful laboratory production of new materials from semimetal and metal powders to the level of efficient industrial applications is, however, fairly slow. This can be explained by substantial difficulties in controlling MW sintering, and that may be related to the fact that physical mechanisms behind this technology are still not fully understood [3], [4].

The interest in practical instruments for specific characterization of the process of MW sintering raises demand on the techniques of testing/monitoring the state of powder samples at different temperatures. Aiming to create the tools capable of producing systematic characteristics of the processes of MW sintering, this goal has been recently attacked from the viewpoint of macroscopic modeling [5]-[8]. However, these models are based on severe idealizations and do not account for the full picture of MW sintering as a complex multiphysics phenomenon coupling electromagnetic, thermal and mechanical processes. Application of conventional *in situ* measurement techniques using different types of sensors and probes (see, e.g., [9]) is very limited here because of high (up to hundreds degrees Celsius) temperatures in the furnace and intrinsic nonuniformity of microwave thermal processing. This motivates the development of suitable means of nondestructive evaluation (NDE) of powder samples under microwave irradiation. A sophisticated technique based on a time-resolved synchrotron radiation and X-ray diffraction [10] provides high-resolution visualization of structural and microstructural changes of materials during MW heating. However, this technique requires highly complicated and very expensive instrumentation and thus unlikely can be widely used for the related experimental studies. This suggests that much simpler (and not necessarily as precise as [10]) techniques for practical NDE may be useful for routine characterization of metal powders in the course of sintering in applied MW systems.

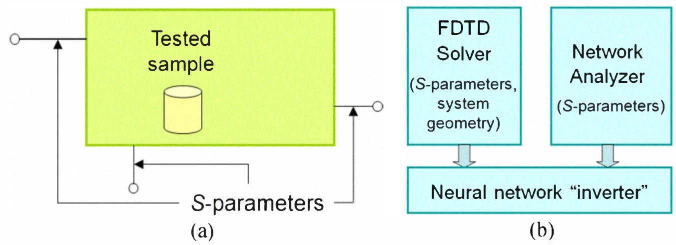

Fig. 1. Conceptual scheme of the NDE technique.

In this paper, we report on the initial steps in the development of an imaging technology for evaluation of inner structure of the powder sample from elementary measurements of *S*-parameters. The proposed technique originates from the concept of modeling-based NDE in closed systems [11]-[12] and relies on the observation that, from a macroscopic modeling prospective, the sintered metal powder cannot be characterized in terms of gradual changes of its effective complex permittivity ε_{eff} and permeability μ_{eff} in the full temperature range. In contrast to ceramic powders, the no-phase-change assumption is not applicable here: at certain temperatures, sizable pieces of bulk metal are formed and grow within powder samples. In response to this feature, the current version of our NDE technique is designed to detect a position and size of a spherical metal inclusion in a powder sample characterized by ε_{eff} and μ_{eff} and situated in a waveguide.

A principal idea of the proposed technique is illustrated in Fig. 1. The approach is based on the application of an artificial neural network (ANN) used for inversion of the problem and reconstruction of the radius and spatial coordinates of the sphere. The *S*-parameters come to the "inverter" from both a numerical (FDTD) electromagnetic analysis of the entire MW system for multiple values of reconstructed parameters and a

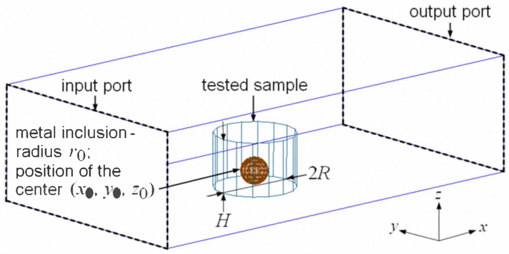

Fig. 2. Microwave two-port system containing a cylindrical powder sample with a metal spherical inclusion.

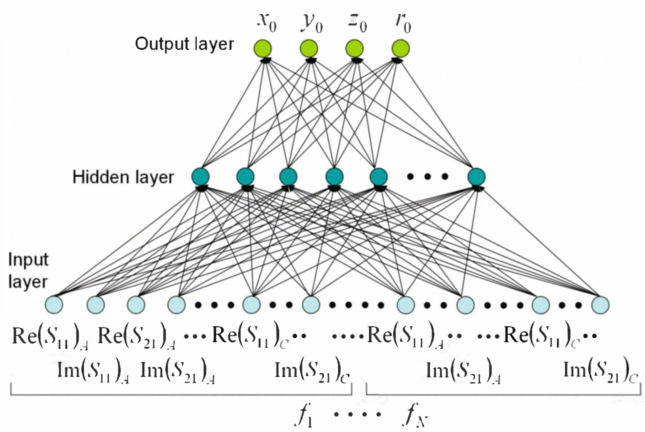

Fig. 3. Architecture of the ANN for reconstruction of spatial coordinates and a radius of a metal sphere.

measurement performed at a particular instance of the sintering processes. The functionality of the technique is demonstrated by a computational test in reconstructing the parameters of a metal sphere in a cylindrical sample of iron powder in a rectangular waveguide.

II. Method

The modeling-based NDE technique for detecting the emerging metal spherical inclusion in the sample of metal powder is realized for a two-port closed system. The measurable characteristics used for monitoring the internal structure of the sample are complex *S*-parameters (the reflection and transmission coefficients, S_{11} and S_{21} respectively) which are determined (computationally and experimentally) in the same ports which are used to input MW energy in the system. The sample is supposed to be fully specified in terms of its material parameters (i.e., $\varepsilon_{\mathrm{eff}}$ and μ_{eff}) and configuration. In this paper, we consider the scenario consisting of a rectangular waveguide and a cylindrical sample staying on its wide wall and containing a metal sphere as shown in Fig. 2.

The aim of the proposed technique is to locate the 3-D coordinates and radius of the inclusion. It has been found from the preliminary computational experiments that in waveguide-type structures *S*-parameters are mostly sensitive to the

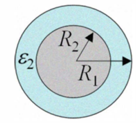

Fig. 4. Structure if a core-shell particle.

position of the inclusion with respect to the position of the sample only along the direction of field propagation, i.e. the *x*-axis. This suggests that in order to retrieve information about location of the sphere in all three coordinates, one can deal with *S*-parameters corresponding to three orientations of the sample rotated by 90° with respect to each other when the second position of the sample is rotated around the *z*-axis and the third position is obtained by rotating around the *y*-axis. In contrast to the approach outlined in [11], here, in order to increase the amount of input information and improve precision of reconstruction, we use *S*-parameters obtained for a number of frequencies in an interval (f_1, f_2) around the working frequency of MW thermal processing f_0. (This approach presumes that *S*-parameters are measured by a suitable high power network analyzer (see, e.g., [13]).)

Parameters of the sphere are reconstructed with the use of a radial basis function (RBF) ANN shown in Fig. 3. The ANN *F* approximates the map $\mathscr{F}: X \rightarrow Y$, where *X* is a vector of size $(12\times N)\times 1$ whose elements are real and imaginary parts of the reflection and transmission coefficients, *Y* is a vector of size 4×1 that consists of the coordinates of the center (x_0, y_0, z_0) and radius (r_0) of the inclusion, and *N* is the number of frequency points.

It is supposed that for any allowable set of reconstructed parameters, frequency responses of *S*-parameters can be obtained from numerical simulation. With the help of an electromagnetic solver, we generate *P* samples of input-output pairs and use them for training the ANN. The RBF is chosen to be a cubic basis function given by $\phi_k(X) = ||X - \mathbf{c}_k||^3$, where $\mathbf{c}_k$ is the center of the RBF and the centers are chosen to be the training inputs **X**. Essentially, *F* is a linear combination of *P* cubic RBFs.

The training numerical data is found with the use of full-wave 3-D conformal FDTD simulator *QuickWave-3D* [14]. The output training points are chosen as random combinations of positions and radii uniformly distributed in the specified domain. When the ANN is sufficiently well trained by modeling data, it is able to reconstruct the parameters of the sphere using the *S*-parameters obtained from the related measurement.

III. Results

The numerical results presented in this section are obtained for the cylindrical sample with $R = 15$ mm and $H = 20$ mm that is located in the center of the wide wall. The material of the sample is powder of core-shell particles randomly distributed in air; its effective permittivity and permeability are taken as the ones of iron powder that are estimated, in accordance with

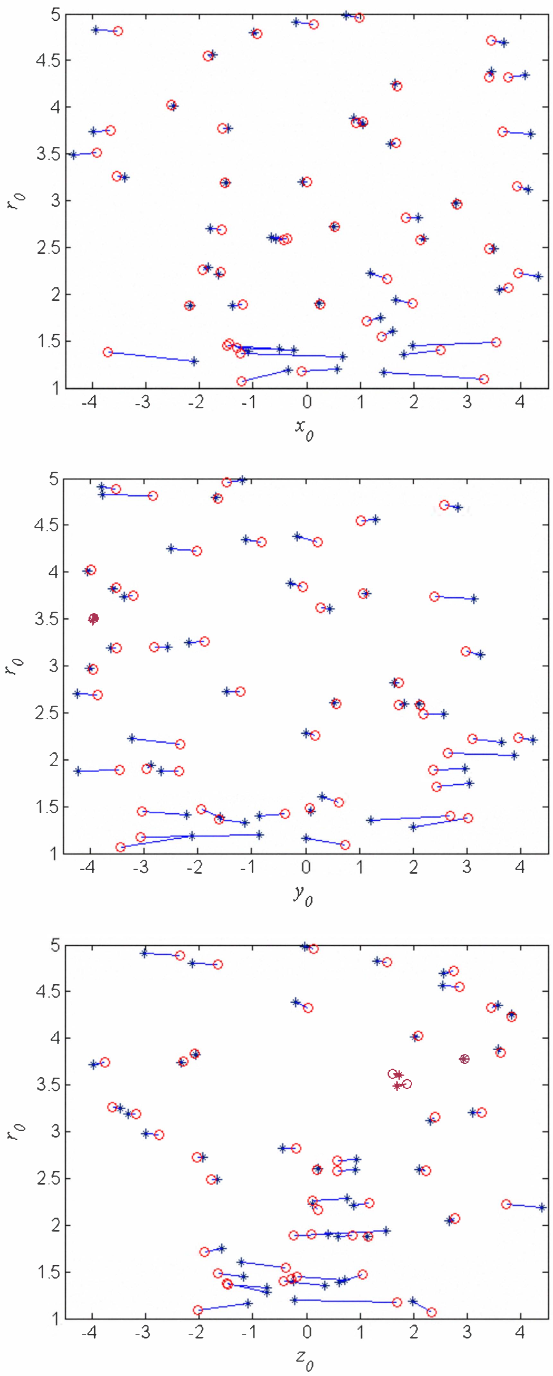

Fig. 5. Parameters of the metal sphere found by the RBF ANN (*) in response to 50 testing points (o); number of training points is 475.

the model [15], to be $\varepsilon_{eff} = 2.25 - j0.000002$ and $\mu_{eff} = 1.0 - j0$. These values correspond to the effective permittivity of crystal lattice of metal core and permittivity of dielectric shell $\varepsilon_1 = 12.0 - j0$ and $\varepsilon_2 = 4.0 - j0$, respectively, the core-shell proportion $(R_2 - R_1)/R_1 = 0.1$ (with R_2 and R_1 being the external radii of the shell and the core, respectively, as shown

TABLE I

RECONSTRUCTED PARAMETERS OF A METAL SPHERE IN A CYLINDRICAL SAMPLE OF IRON POWDER

S	*Position & radius*	x_0	y_0	z_0	r_0
1	actual	-4.0	-4.0	0	3.0
	reconstructed	-4.62	-4.37	0.02	2.96
	error, %	**3.2**	**1.8**	**0.1**	**0.2**
2	actual	2.0	-2.0	-2.0	3.0
	reconstructed	2.27	-2.28	-2.12	3.02
	error, %	**1.4**	**1.4**	**0.6**	**0.1**
3	actual	1.0	1.0	1.0	4.0
	reconstructed	1.24	1.19	0.87	4.04
	error, %	**1.2**	**0.9**	**0.7**	**0.2**
4	actual	0.0	3.0	2.0	5.0
	reconstructed	0.18	3.44	2.47	4.95
	error, %	**0.9**	**2.1**	**2.4**	**0.2**
Average error (12 tests), %		**1.9**	**2.2**	**1.3**	**0.2**

on Fig. 4), and the volume fraction of core-shell particles in the sample 0.2.

Since many of applied systems of MW thermal processing operate at f_0 = 2.45 GHz, we adopt it as a frequency at which MW sintering is performed and which is within the interval (f_1, f_2). For sake of simplicity and in order to reduce computational cost of the study, we choose a two-port closed system to be a section of the WR340 waveguide (86 × 34 × 250 mm); the frequency interval is taken to be bounded by f_1 = 2 GHz and f_2 = 3 GHz and having N = 21.

Numerical data were obtained using a fine FDTD model of the entire system that contains 60,000 to 70,000 cells (depending on the orientation of the sample and the size of the sphere) with the smallest ones of 0.8 mm. The steady state is reached within about 15,000 time steps, and it takes 1.5-2 min of CPU time of an AMD Athlon 2.2 GHz processor PC.

The parameters to be determined in the reconstruction are sought in the following intervals:

$$1 \le r_0 \le 5 \text{ mm}, -4 \le x_0 \le 4 \text{ mm}, -4 \le y_0 \le 4 \text{ mm}, -4 \le z_0 \le 4 \text{ mm},$$

where the spatial coordinates are measured with respect to the center of the cylinder.

The performance of the trained network is illustrated in Fig. 5. The technique finds the parameters of the sphere with a sufficiently high resolution when the network responses are close to the test points, i.e., for the spheres with radii greater than 1.5-2.0 mm. Table 1 gives a numerical comparison of the reconstructed parameters of the sphere with their actual values; the average error for 12 test spheres (computed as the sum of relative errors for all cases divided by 12) does not exceed 2.2 %.

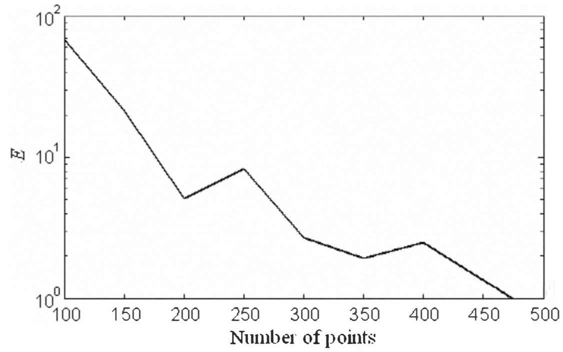

Fig. 6. Average error of reconstruction E versus the number of training points.

Finally, we characterize the accuracy of the technique in the presented illustration by the average total squared error:

$$E = \frac{1}{50}\sum_{i=1}^{50}\left\{\left[x_{0a}^{(i)} - x_{0n}^{(1)}\right]^2 + \left[y_{0a}^{(i)} - y_{0n}^{(1)}\right]^2 + \left[z_{0a}^{(i)} - z_{0n}^{(1)}\right]^2 + \left[r_{0a}^{(i)} - r_{0n}^{(1)}\right]^2\right\},$$

where the squared differences are summarized for 50 randomly taken test points and the indices a and n denote the actual and reconstructed parameters respectively. It is seen from Fig. 6 that the algorithm converges with the number of training points increasing up to 350-400.

IV. Conclusion

A modeling-based technique for detection of a position and size of a bulk metal spherical inclusion emerging in a sample of metal powder in the course of MW sintering has been presented. The numerical test performed for the cylindrical sample of iron powder in a two-port waveguide system shows that the technique allows for fairly precise determining the parameters of the sphere. The reconstruction error depends on the radius; for spheres with r_0 more than ~2 mm, the average errors in getting the position of the center and the radius are 1.8 % and 0.2 % respectively.

The technique presented here for a two-port waveguide system, a cylindrical sample and a spherical piece of sintered metal powder can be straightforwardly upgraded to be applicable to practical (multi-port, geometrically complex) systems for MW sintering, powder samples of other configurations, and inclusions of alternative shapes (e.g., rectangular, ellipsoidal, etc.). Future development of this NDE technology may require refinement of its resolution towards smaller detectable inclusion and resolution of the issue of generation of "non-uniform" numerical data for MW systems with dramatically varying material parameters in order to ensure a stable operation of the ANN "inverter".

V. Acknowledgment

This work was partially supported by the EADS Company Foundation. The authors are grateful to Sébastien Vaucher for discussions of motivation for this study.

References

[1] D.E. Clark and W.H. Sutton, "Microwave processing of materials," *Annu. Rev. Mater. Sci.*, vol. 26, pp. 299-331, 1996.

[2] D. Agrawal, J. Cheng, Y. Fang, and R. Roy, "Microwave processing of ceramics, composites and metallic materials," in *Microwave Solutions for Ceramic Engineers*, D.E. Clark, D.C. Folz, C.E. Folgar, and M.M. Mahmoud, Eds., Westerville, OH: Amer. Ceram. Soc. Publ., pp. 205-228, 2005.

[3] M. Gupta and E.W.W. Leong, *Microwaves and Metals,* Singapore: John Wile & Sons (Asia), 2007.

[4] A. Mondal, D. Agrawal, and A. Upadhyaya, "Microwave heating of pure copper powder with varying particle size and porosity," *J. Microw. Power & Electromagn. Energy*, vol. 43, no. 1, pp. 5-10, 2009.

[5] P. Mishra, G. Sethi, and A. Upadhyaya, "Modeling of microwave heating of particulate metals," *Metallurgical and Materials Trans. B*, vol. 37B, pp. 839-845, 2006.

[6] Y. Duan, D.C. Sorescu, and J.K. Johnson, "Finite element approach to microwave sintering of oxide materials," *Proc. of the COMSOL Users Conference, Boston, 2006.*

[7] V.D. Buchelnikov, D.V. Louzguine-Luzgin, A.P. Anzulevich, I. V. Bychkov, N. Yoshikawa, M. Sato, and A. Inoue, "Modeling of microwave heating of metallic powders," *Physica B*, vol. 403, pp. 4053-4058, 2008.

[8] M. Ignatenko, M. Tanaka, and M. Sato, "Numerical analysis of microwave heating of copper powders," *Proc. 12th AMPERE Microwave High Frequency Heating Conf.,* Karlsruhe, Germany, 2009, pp. 206-209.

[9] R.D. Peelamedu, D.C. Dube, M.T. Lanagan, and D. Agrawal, "*In situ* probing of magnetic parameter variations of nickel zinc ferrites during microwave *H* heating," *Applied Physics Lett.*, vol. 88, 204108, 2006.

[10] S. Vaucher, "Time-resolved imaging of material changes under microwave irradiation," *2009 IEEE MTT-S Int. Microwave Symp. Workshop "Recent Advances in Microwave Power Applications & Techniques (RAMPAnT)*," June 2009.

[11] A.V. Brovko, E.K. Murphy, M. Rother, H.P. Schuchmann, and V.V. Yakovlev, "Waveguide microwave imaging: spherical inclusion in a dielectric sample," *IEEE Microwave & Wireless Components Lett.*, vol. 18, no 9, pp. 647-649, 2008.

[12] A.V. Brovko, E.K. Murphy, and V.V. Yakovlev, "Waveguide microwave imaging: neural network reconstruction of functional 2-D permittivity profiles," *IEEE Trans. Microw. Theory Tech*, vol. 57, no. 2, pp. 406-414, 2009.

[13] J.-M. Catalá-Civera and F. Peñaranda-Foix, "Advanced microwave measurements for high-power applications," *2009 IEEE MTT-S Int. Microwave Symp. Workshop "Recent Advances in Microwave Power Applications & Techniques (RAMPAnT)*," June 2009.

[14] *QuickWave-3D*TM, QWED Sp. z o.o., ul. Nowowiejska 28, lok. 32, 02-010 Warsaw, Poland, http://www.qwed.com.pl/.

[15] V.D. Buchelnikov, D.V. Louzguine-Luzgin, G. Xie, S. Li, N. Yoshikawa, M. Sato, A.P. Anzulevich, I.V. Bychkov, and A. Inoue, "Heating of metallic powders by microwaves: experiment and theory," *J. Applied Physics*, vol. 104, 2008.